This article has been accepted for publication in a future issue of this journal, but has not been fully edited. Content may change prior to final publication. Citation information: DOI 10.1109/TMC.2014.2338293, IEEE Transactions on Mobile Computing

Game-theoretic Topology Control for Opportunistic Localization in Sparse Underwater Sensor Networks

Sudip Misra, *Senior Member, IEEE,* Tamoghna Ojha, *Student Member, IEEE,* Ayan Mondal, *Student Member, IEEE*

Abstract— In this paper, we propose a localization scheme named Opportunistic Localization by Topology Control (OLTC), specifically for sparse Underwater Sensor Networks (UWSNs). In a UWSN, an unlocalized sensor node finds its location by utilizing the spatio-temporal relation with the reference nodes. Generally, UWSNs are sparsely deployed because of the high implementation cost, and unfortunately, the network topology experiences partitioning due to the effect of passive node mobility. Consequently, most of the underwater sensor nodes lack the required number of reference nodes for localization in underwater environments. The existing literature is deficient in addressing the problem of node localization in the above mentioned scenario. Antagonistically, however, we promote that even in such sparse UWSN context, it is possible to localize the nodes by exploiting their available opportunities. We formulate a game-theoretic model based on the *Single-Leader-Multi-Follower Stackelberg game* for topology control of the unlocalized and localized nodes. We also prove that both the players choose strategies to reach a *socially optimal Stackelberg-Nash-Cournot Equilibrium*. NS-3 based simulation results indicate that the localization coverage of the network increases upto 1.5 times compared to the existing state-of-the-art. The energy-efficiency of OLTC has also been established.

Index Terms—Opportunistic Localization, Game Theory, Topology Control, Sparse UWSNs, Oligopoly

1 Introduction

1.1 Motivation

Localization of sensor nodes is fundamentally important in event-driven sensor networks [1]–[4]. In such networks, the sensed data render meaningful insights when they are tagged with location information. Location-awareness is required in applications such as target tracking [5], [6], ocean monitoring, pollution control, or even for the execution of geographic routing protocols [7]. However, UWSNs pose few unique challenges that differ from those of the terrestrial sensor networks in many respects [8]–[10]. Unlike the terrestrial networks, Global Positioning System (GPS) is unsuitable for use in underwater environments due to high attenuation of radio signal. Also, the power-hungry nature of GPS makes it inappropriate for use in UWSNs. Alternatively, in UWSNs, location of a sensor node is determined by utilizing its spatio-temporal relation with the reference nodes. In many UWSN applications such as underwater surveillance, the nodes are sparsely deployed because of the high deployment cost [11]. Further, the presence of passive node mobility due to underwater currents renders spatio-temporal partitioning of the network topology. Consequently, most of the underwater sensor nodes lack the availability of required number of reference nodes in their communication range for aiding in localization. Also, the neighborhood of a node may change over time, and accordingly, the number of available reference nodes may also change.

The existing works (e.g. [12]–[20]) on underwater localization considered various constraints of UWSNs *except* the sparse and network partitioning scenarios. Ref. [21] considers a scenario which requires at least three anchors for initiating the localization process. The lack of required number of reference nodes or the variability of the available reference nodes affects the execution of any localization scheme. The existing localization schemes are broadly classified into two categories – *anchor-based* and *anchor-free*. The anchor-based schemes perform localization iteratively starting from the surface based anchors. Unfortunately, these schemes fail to function in sparse and partitioned deployment scenarios. On the other hand, anchor-free schemes use mobile beacon nodes (such as AUVs and DNR-beacons) to aid node localization. These additional devices increase the implementation cost of these schemes. Furthermore, these schemes exhibit performance challenges attributed to low success rate in sparse UWSNs. Therefore, it is required to design a scheme which is capable of localizing the sensor nodes by exploiting the available opportunities to fulfil the required number of reference

- *The authors are with the School of Information Technology, Indian Institute of Technology Kharagpur, WB, 721302, India. E-mail: {smisra, tojha, ayanmondal}@sit.iitkgp.ernet.in*

- *This work is partially supported by a grant from the Department of Electronics and Information Technology, Government of India, Grant No. 13(10)/2009-CC-BT, which the authors gratefully acknowledge.*

This article has been accepted for publication in a future issue of this journal, but has not been fully edited. Content may change prior to final publication. Citation information: DOI 10.1109/TMC.2014.2338293, IEEE Transactions on Mobile Computing

nodes in sparse UWSNs.

1.2 Contributions

In this paper, we propose *Opportunistic Localization by Topology Control* (*OLTC*), a localization scheme specifically designed for sparse and partitioned UWSNs. In OLTC, we depict the interaction between an unlocalized node and surrounding localized nodes (the potential reference nodes) as an oligopoly. We model the scenario as a *Single-Leader-Multi-Follower Stackelberg game*, where any unlocalized node acts as the leader, and any localized node acts as the follower. In such oligopolistic environment, the unlocalized node is referred to as the *Stackelberg firm*, by following the nomenclature used in micro-economic games [22]. Further, the existing localized nodes, which help an unlocalized node to localize it, are referred to as the *Cournot firms*. Any unlocalized node exploits its *available opportunities* to interact with potential reference nodes to get localized with minimum localization delay. The localized nodes, on the other hand, decide an optimal transmission power to maximize their individual utility. In summary, the *contributions* of this work are as follows.

- We formulate the interaction between an unlocalized node and potential reference nodes (localized nodes) as a Single-Leader-Multi-Follower Stackelberg game. This game model establishes the broader scope for opportunistic localization in sparsely deployed UWSNs by instrumenting topology control mechanisms.
- We propose a model for the unlocalized nodes to exploit the possibilities of opportunistic localization — a mechanism that helps in addressing the challenge of finding maximum available reference nodes.
- We present an on-demand, topology controlled location beacon providing scheme for the one-time localized nodes, which act as potential anchors for the rest of the unlocalized nodes. This fabric is usable for enforcing power-awareness in the localization process.

The paper is organized as follows. In Section 2, we briefly present the existing literature in the area of UWSN localization and topology control in sensor networks. The system model is discussed in Section 3. The proposed OLTC framework is described in Section 4. We analyze the simulation results of the proposed scheme in Section 5. Finally, in Section 6, the paper concludes by citing directions for future work.

2 Related Works

2.1 Localization in UWSNs

In recent years, a number of research works investigated the problem of node localization in UWSNs. Ref. [2], [3] survey these works in detail. Among the iterative schemes, the Three Dimensional Localization Algorithm for Underwater Acoustic Sensor Networks (3DUL) [12] presents a localization approach in which location estimation propagates starting from the surface-based anchor nodes. The unlocalized nodes and the anchors perform two-way message exchange to estimate the intermediate distance and the anchor node's coordinate. The unlocalized node estimates its location based on the trilateration scheme. However, in 3DUL, the sensor nodes are considered to be stationary.

The effect of node mobility was considered in the Scalable Localization with Mobility Prediction (SLMP) [13] scheme. The authors consider an architecture consisting of surface buoys, anchor nodes, and ordinary nodes. The anchor nodes estimate their future coordinates based on their past coordinates and predicted mobility pattern. These anchors also calculate their coordinates using the lateration technique with reference to the surface buoys. The anchors assume their predicted mobility pattern to be valid, if the difference between the calculated and the estimated coordinates is less than a threshold value. Otherwise, the mobility pattern is updated. The ordinary nodes calculate their location and mobility pattern by listening to the updates from the anchor nodes. However, in this scheme, the anchor nodes perform long distance acoustic communication with the surface buoys, and node density is assumed to be high.

Localization schemes proposed in Refs. [21] and [15] transform the localization problem from 3-dimension (3D) to 2-dimension (2D), with the use of depth and projection informations. A sensor node estimates its location using the projected anchor nodes. However, if location estimation by these anchor nodes fails, the unlocalized node waits for another anchor's beacons. Localization Scheme for Large Scale underwater networks (LSLS) [23] and Underwater Positioning System (UPS) [14] were proposed for stationary UWSNs. In these schemes, the location is estimated with the help of reference nodes, and then it is repeated iteratively.

Erol *et al.* proposed a surface anchor-free localization scheme named Dive'N'Rise Localization (DNRL) [16] which uses Dive'N'Rise beacons (DNR-beacons). These mobile DNR-beacons get their GPS coordinates while floating, and then dive inside water to aid the localization of the sensor nodes. The advantage of this scheme is that it is 'silent', and energy-efficient. However, the slow descending speed of the DNR-beacons increase the location estimation errors in the presence of node mobility. Also, large number of DNR-beacons are required for large-scale networks, thereby increasing the implementation cost of the network. AUVs were used as beacon nodes in few schemes [17]–[19]. In addition to incurring additional cost to the network, the localization success of these schemes greatly depend on the trajectory of the AUV.

All these schemes proposed for UWSN localization considered various constraints of UWSN, except explicitly the sparse and partitioned deployment scenarios, where the unlocalized nodes lack the required number of

This article has been accepted for publication in a future issue of this journal, but has not been fully edited. Content may change prior to final publication. Citation information: DOI 10.1109/TMC.2014.2338293, IEEE Transactions on Mobile Computing

reference nodes. In such cases, the existing anchor-based localization schemes [12], [15], [20], [21], [23] exhibit limited localization coverage. The AUV-based schemes may be considered alternatively. However, these require the knowledge of the deployment area, which increases the overall implementation and deployment cost.

2.2 Topology Control

The approach for topology control was taken in various complementary ways, including medium access and routing, to extend the lifetime of a network [24], [25]. The topology control scheme presented in DRNG [24], DLSS [24] and STC [26] start with neighbor finding, where all the nodes transmit at their maximum power. Later, each node computes the minimum transmission power required to maintain network connectivity. Another decentralized topology control scheme, which considered both connectivity and frame success rate, was proposed in [27] based on a complete information game. Recently, more such schemes based on game-theory were proposed. Ref. [28] takes into account cross-layer information such as signal-to-interference-plus-noise (SINR) and MAC/network layer connectivity to optimally allocate transmission power for nodes. The changes in the residual energy of the nodes was considered in [25] for framing a game-theoretic model of the topology control scheme. There exist few works on topology control in UWSNs as well. Liu *et al.* [29] proposed a scheme which considers the anchored nodes present in UWSNs. However, the authors did not consider the energy consumption incurred due to receiving of messages. Ojha *et al.* [30] proposed a 'virtual topology' to maintain the connectivity among the nodes from sea-bed to sea-surface. However, the scheme is not suitable for sparse and partitioned networks.

2.3 Synthesis

The analysis of the existing literature reveals that topology control is applied in solving different problems such as finding optimal transmission range to maintain network connectivity, minimization of node's energy consumption with cross-layer information, or selection of the minimum set of active nodes. In contrast to the above-cited works (e.g. [27], [26], [25]), in this paper, we leverage the benefits of topology control for better node localization, specifically in sparse deployment scenarios. To the best of our knowledge, this is a formative work which introduces the idea of using topology control mechanisms to solve the problem of localization in UWSNs. Further, we emphasize that the problem instance of node localization considered in our study — a single unlocalized node needing multiple localized neighbor nodes to successfully localized itself — motivates the use of single-leader-multi-follower analytical model. This game-based solution proposed in our work enables the establishment of *opportunistic localization* in *sparsely deployed* UWSNs, as explained elaborately in Section 4.3. It may be clarified that the attributes of opportunism in localization and the consideration of sparse deployment scenario make the proposed solution distinct from the existing similar works on topology control ([27], [26], [25]).

3 System Model and Assumptions

We assume a 3D UWSN consisting of mobile nodes (N) represented as a graph $G(N, E(t))$, which are affected by passive node mobility due to waves and underwater currents. For any node i, $\{Nbr(i)\}_{p_i}$ denotes the set of its neighbors for transmission power p_i, and $P_i(t)$ denotes the action space of available power levels at time t. Initially, all the nodes transmit in the same and minimum power level p_{min}. Here, the minimum transmission power is $p_{min} = \inf(P_i(\cdot))$ and maximum transmission power is $p_{max} = \sup(P_i(\cdot))$ for any node i. Changing the power level of a node corresponds to changing its transmission range. Let $R_i(t)$ represent the set of transmission ranges of a node at time t. Therefore, $P_i(\cdot)$ and $R_i(\cdot)$ possess an one-to-one bijective mapping, i.e., $f : P_i(\cdot) \rightarrow R_i(\cdot)$. Accordingly, $P_i(\cdot) = [p_1, p_2, \cdots, p_\kappa]$ and $R_i(\cdot) = [r_1, r_2, \cdots, r_\kappa]$, where κ is the number of transmission power levels, and it is defined as $\kappa = |P_i(\cdot)|$, where $|\cdot|$ denotes the cardinality of a set. In the assumed deployment, $j \in \{Nbr(i)\}_{p_i}$ in the network graph $G(N, E(t))$ *iff* $(i, j) \in E(t)$, and the distance between i and j is $d_{ij} \leq r_i$ for $r_i \in R_i(\cdot)$. As depicted in Figure 1, whereas the unlocalized nodes are submerged into water throughout the network, the localized sensor nodes or anchors are positioned on the water surface. The dotted circles in Figure 1 show the area covered by the nodes with transmission range $r_i = r_{min}$. Table 1 lists the symbols used in the paper.

3.1 Assumptions

We list the assumptions made in the design of the proposed work.

- A sensor node is aware of its depth.
- Nodes are time-synchronized.
- They have knowledge about various cross-layer information such as topology, connectivity, and residual battery status.
- Anchor nodes, which act as initial reference nodes, are deployed on the water surface.

4 Opportunistic Localization by Topology Control (OLTC)

4.1 Why Single-Leader-Multi-Follower Stackelberg game?

In a distributed localization scenario, an unlocalized node is able to successfully localize itself after receiving location beacons from multiple localized nodes. However, due to the presence of sparseness in node deployment, reception of location beacons from multiple

This article has been accepted for publication in a future issue of this journal, but has not been fully edited. Content may change prior to final publication. Citation information: DOI 10.1109/TMC.2014.2338293, IEEE Transactions on Mobile Computing

TABLE 1: List of Symbols

Symbol	Meaning
N	The set of all nodes
N_l	The set of the localized nodes
N_{ul}	The set of the unlocalized nodes
$E(t)$	The set of the edges in the network
$Nbr(i)_{p_i}$	The set of the neighbors of node i for transmission power p_i
p_i	The transmission power of node i
$P_i(t)$	The set of available transmission power levels of node i at time t
p_{min}	Minimum transmission power of any node
p_{max}	Maximum transmission power of any node
r_i	The transmission range of node i
$R_i(t)$	The set of available transmission range levels of node i at time t
r_{min}	Minimum transmission range of any node
r_{max}	Maximum transmission range of any node
$W(t)$	The set of total residual energy of nodes at time t
$\mathcal{U}_j$	Utility of localized node $j \in N_l$
Ψ_i	Utility of unlocalized node $i \in N_{ul}$
OPR_i	Opportunistic region of node i
$MaxOPR_i$	Maximum opportunistic region of node i
$\mathcal{P}_i$	Profit of node i
$\mathcal{A}_i^{RR}$	Ability of a localized node i to resolve requests
$\mathcal{A}_i^{SD}$	Ability of a localized node i to serve demands
n_{OReq}	Number of opportunity request messages received
$n_{OReq}^{p_i}$	Number of opportunity requests that can be resolved by node i with transmission power p_i
n_{ref}^k	*Additional* number of reference nodes required to localize node k
$n_{ref}\|_{max}$	The number of reference nodes required for a node to get localize
$\{J\}_{p_i}$	The set of localized neighbors of node i for transmission power p_i
t_{delay}	Localization delay
d_{ij}	Distance between node i and j

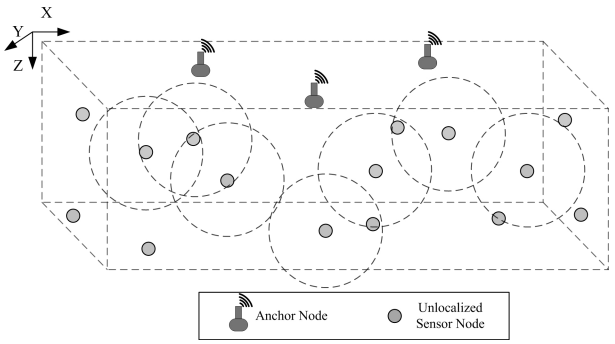

Fig. 1: Deployment scenario of OLTC

localized neighbors may not be achieved[1]. In such a scenario, the unlocalized nodes initiate the localization process, and the localized nodes follow the process by replying with beacons. Thereby, we use *Single-Leader-Multi-Follower Stackelberg game* [22], where the unlocalized node acts as the *single leader*, and the localized nodes are the *multiple followers*. This interaction is termed as an 'oligopolistic market', as in such market environment there are limited number of players.

Therefore, by exploiting topology control, the unlocalized nodes are able to interact with more localized nodes, and further request them for location beacons. On the other hand, the localized nodes also perform topology control to maximize the number of unlocalized nodes they interact with while minimizing the energy consumption. These nodes select an optimal transmission power with the help of the Single-Leader-Multi-Follower Stackelberg game. We describe the game formulation for performing topology control of the nodes in Section 4.2. In Theorem 4.1, we prove the effectiveness of adopting the Stackelberg game formulation to perform topology control.

Theorem 1. *The energy consumption of the sensor nodes for performing localization with the Single-Leader-Multi-Follower Stackelberg game is less than the case when no game is used. Mathematically,*

$$\bar{\mathcal{E}} < \mathcal{E} \tag{1}$$

where

$\bar{\mathcal{E}}$: *Total energy consumption by* ***using the said game***
$\mathcal{E}$: *Total energy consumption by* ***not using the said game***

Proof: Let us consider two different scenarios for localization — with and without the Single-Leader-Multi-Follower Stackelberg game. We also assume that same number of nodes is localized in both the scenarios. The transmission power of any localized node is $p_i \leq p_{max}$, and $\mathcal{E}_i(\cdot)$ and $\bar{\mathcal{E}}_i(\cdot)$ denote the energy consumption of node i for the scenarios without game and with game, respectively.

If we *do not* use the Single-Leader-Multi-Follower Stackelberg game, all localized nodes have transmission power $= p_{max}$. Therefore, the total consumed energy for transmission is,

$$\mathcal{E} = \sum_{i=0}^{|N_l|} \mathcal{E}_i(p_{max}) \tag{2}$$

On the other hand, by using the Single-Leader-Multi-Follower Stackelberg game, a set of localized nodes $\bar{N}_l \subseteq N_l$ are able to localize the same number of unlocalized nodes with transmission power $\bar{p}_i$, where $i \in \bar{N}_l$ and $\bar{p}_i < p_{max}$. In this case, the overall energy consumption is,

$$\bar{\mathcal{E}} = \sum_{i=0}^{|\bar{N}_l|} \bar{\mathcal{E}}_i(\bar{p}_i) + \sum_{i=0}^{|N_l|-|\bar{N}_l|} \mathcal{E}_i(p_{max}) \tag{3}$$

Therefore, it is straightforward to verify that $\bar{\mathcal{E}} < \mathcal{E}$. Hence, using the Single-Leader-Multi-Follower Stackelberg game, the sensor nodes maintain energy-efficiency. □

4.2 Topology Control with Single-Leader-Multi-Follower Stackelberg Game

We model the interaction between the localized and the unlocalized nodes as a Single-Leader-Multi-Follower

1. It is noteworthy that even in sparse UWSNs, the regular functionalities of sensing and multi-hop communication to the surface sinks can be performed. The challenge in localization in UWSNs is due to the requirement of a minimum set of reference nodes.

This article has been accepted for publication in a future issue of this journal, but has not been fully edited. Content may change prior to final publication. Citation information: DOI 10.1109/TMC.2014.2338293, IEEE Transactions on Mobile Computing

Stackelberg game [22], as discussed in Section 4.1. The followers seek to maximize their individual benefit during 'Opportunistic Localization' in a non-cooperative manner. Furthermore, an unlocalized node seeks to maximize its own profit while considering the response of the followers (the localized nodes). Thus, in an oligopolistic environment, the followers are *Cournot firms* and the leader is the *Stackelberg firm*. We define the game in its strategic form as $\mathcal{G} = \langle \{N_l \cup N_{ul}\}, P(t), W(t), \{\mathcal{U}_l\}_{l \in N_{ul}}, \{\mathcal{U}_f\}_{f \in N_l} \rangle$, with the following components:

- The set of localized nodes, N_l.
- The set of unlocalized nodes, N_{ul}.
- The set of total action space (power level) at time t, $P(t) = \{P_1(t), P_2(t), \cdots, P_i(t), \cdots, P_n(t)\}\ \forall i \in N$.
- The set of total residual energy of nodes at time t, $W(t)$.
- The set of utility functions for follower, $\{\mathcal{U}_f\}_{f \in N_l}$.
- The set of utility functions for leader, $\{\Psi_l\}_{l \in N_{ul}}$.

Definition 1. *The Opportunistic Region ($\mathbf{OPR_i}$) of a node i is defined as the region covered by it for transmission power $p_i < p_{OPR} < p_{max}$, where p_i is the current transmission power of node i.*

Definition 2. *The Maximum Opportunistic Region ($\mathbf{MaxOPR_i}$) of a node i is the region covered by it for transmission power $p_{OPR} = p_{max}$.*

Definition 3. *The profit ($\mathcal{P}_i(\cdot)$) of a sensor node i is defined as the difference between the revenue ($\mathcal{R}_i(\cdot)$) generated and the cost ($\mathcal{C}_i(\cdot)$) incurred.*

$$\mathcal{P}_i(\cdot) = \mathcal{R}_i(\cdot) - \mathcal{C}_i(\cdot) \tag{4}$$

In our works, $\mathcal{R}_i(\cdot)$ and $\mathcal{C}_i(\cdot)$ are representative of the Ability and energy consumption of the node i.

4.2.1 Utility function for Localized Nodes

The localized nodes are the followers ($f \in N_l$) of the oligopolistic market. They decide their strategy to localize maximum number of nodes with minimum energy consumption. In the following, we define the rules for utility calculation of these followers.

i) The utility ($\mathcal{U}_j$) of a follower j is considered to be non-increasing, as with an increase in the transmission power level ($\wp_j = \tilde{p}_j - p_j$), the energy consumption of the localized node becomes higher. Here, $\tilde{p}_j$ and p_j are the new and current power levels, respectively. Thus, the profit ($\mathcal{P}_j(\cdot)$) of a node decreases by choosing higher $\tilde{p}_j$, as mentioned in Lemma 4.2.1. Therefore, the utility is represented mathematically as,

$$\frac{\delta \mathcal{U}_j}{\delta \wp_j} \leq 0 \tag{5}$$

Theorem 2. *For a node, with the increase in the transmission power, the number of localized/unlocalized neighbors is higher or at least equal. Mathematically, $|\{Nbr(\cdot)\}_{p_2}| \geq |\{Nbr(\cdot)\}_{p_1}|$, where $p_2 > p_1$.*

Proof: Let us consider that we have k_1 and k_2 number of localized and unlocalized nodes present in the $\mathbf{OPR_S}$ of a node S.

Thus, $n_2 = n_1 + k_1 + k_2$, where $k_1 \geq 0$ and $k_2 \geq 0$, and $n_1 = |\{Nbr(\cdot)\}_{p_1}|$ and $n_2 = |\{Nbr(\cdot)\}_{p_2}|$ represent the number of nodes present in transmission ranges r_1 and r_2, respectively.

Certainly, $n_2 \geq n_1$, considering any value for k_1 and k_2.

Let, N_1 and N_2 represents the set of nodes present inside r_1 and r_2, respectively. Mathematically, $|N_2 \cap N_l| \geq |N_1 \cap N_l|$ and $|N_2 \cap N_{ul}| \geq |N_1 \cap N_{ul}|$.

Let us assume that the sensor node S has two different transmission power levels, p_1 and p_2. The corresponding transmission ranges are r_1 and r_2, respectively. Therefore, $p_2 > p_1$ and $r_2 > r_1$.

Let us assume that the network has n number of deployed nodes over the region of $d \times d \times d$ size. Thus, N_1, the set of neighbors for transmission range r_1 has $n_1 = \frac{n}{d^3} \times \frac{4}{3}\pi r_1^3$ number of nodes. Similarly, N_2, the set of neighbors for range r_2 has $n_2 = \frac{n}{d^3} \times \frac{4}{3}\pi r_2^3$ number of nodes.

Therefore, considering an uniform deployment of nodes throughout the network, it is straightforward to verify that,

$$n_2 > n_1, \quad \text{if } r_2 > r_1 \tag{6}$$

Equation 6 satisfies for the cases when $k_1 > 0$ and $k_2 \geq 0$, or $k_1 \geq 0$ and $k_2 > 0$.

Hence, the higher the transmission power of a node, the higher (or equal) is the number of localized/unlocalized neighbors of it. □

ii) The transmission range (r) of a localized node increases with the increase in its transmission power (p_j). Consequently, as proved in Theorem 4.2.1, for a localized node, the probability to localize more unlocalized nodes increases. Therefore

$$\frac{\delta \mathcal{U}_j}{\delta \tilde{p}_j} \geq 0 \tag{7}$$

Definition 4. *For any localized node $j \in N_l$, the number of requests that can be resolved is ($n_{OReq}^{\tilde{p}_j}$), with transmission power level ($\tilde{p}_j$) among the total number of 'OReq' packets (n_{OReq}) received. Therefore, the 'ability to resolve requests' ($\mathcal{A}_j^{RR}$) is defined as,*

$$\mathcal{A}_j^{RR} = \frac{n_{OReq}^{\tilde{p}_j}}{n_{OReq}} \tag{8}$$

Definition 5. *The number of localized neighbors of any node i for transmission power p_i is defined as,*

$$\{J\}_{p_i} = |\{Nbr(i)\}_{p_i} \cup N_l| \tag{9}$$

Definition 6. *The **additional** number of reference nodes required for any unlocalized node i to get successfully localized is defined as the difference between the total number of reference nodes required and the number of localized neighbors present,*

$$n_{ref}^i = n_{ref}|_{max} - \{J\}_{p_i} \tag{10}$$

This article has been accepted for publication in a future issue of this journal, but has not been fully edited. Content may change prior to final publication. Citation information: DOI 10.1109/TMC.2014.2338293, IEEE Transactions on Mobile Computing

Definition 7. *The overall demand to any localized node $j \in N_l$ receiving $n_{_{OReq}}$ number of requests is defined by,*

$$\mathcal{D}_j = \sum_{m=1}^{n_{OReq}} n_{ref}^{k} \tag{11}$$

where k is the node ID of the m^{th} OReq message. It is computed as $k = Id[m]$. We assume, $Id[\cdot]$ holds the IDs of the nodes which send the OReq message. Also, $k \in \{Nbr(j)\}_{p_i}$ and $k \in N_{ul}$.

Definition 8. *For any localized node $j \in N_l$ with transmission power $\tilde{p}_j$, only $n_{_{OReq}}^{\tilde{p}_j}$ requests can be served among the total demand of reference nodes ($\mathcal{D}_j$). Thus, the 'ability to serve demand' ($\mathcal{A}_j^{SD}$) is calculated as,*

$$\mathcal{A}_j^{SD} = \frac{n_{_{OReq}}^{\tilde{p}_j}}{\sum_{k=1}^{n_{OReq}} n_{ref}^{k}} \tag{12}$$

Definition 9. *The total 'ability' ($\mathcal{A}_j$) of a localized node $j \in N_l$ is the sum of the 'ability to resolve requests' ($\mathcal{A}_j^{RR}$) from unlocalized nodes, and the 'ability to serve demand' ($\mathcal{A}_j^{SD}$) with its current transmission power level ($\tilde{p}_j$). Mathematically,*

$$\mathcal{A}_j = \mathcal{A}_j^{RR} + \mathcal{A}_j^{SD}$$

$$or,\ \mathcal{A}_j = \frac{n_{_{OReq}}^{\tilde{p}_j}}{n_{_{OReq}}} + \frac{n_{_{OReq}}^{\tilde{p}_j}}{\sum_{k=1}^{n_{OReq}} n_{ref}^{k}} \tag{13}$$

iii) For a specific transmission power level $\tilde{p}_j$, a follower node's (j's) utility increases with an increase in its *ability* to localize more nodes.

$$\frac{\delta \mathcal{U}_j}{\delta \mathcal{A}_j} > 0 \tag{14}$$

Therefore, the overall utility of any follower j is defined as,

$$\mathcal{U}_j = \tan^{-1}(e^{-\frac{\tilde{p}_j - p_j}{p_j}}) + \left(\frac{n_{_{OReq}}^{\tilde{p}_j}}{n_{_{OReq}}} + \frac{n_{_{OReq}}^{\tilde{p}_j}}{\sum_{k=1}^{n_{OReq}} n_{ref}^{k}} \right) \tilde{p}_j \tag{15}$$

Lemma 1. *The profit ($\mathcal{P}_j(\cdot)$) of a localized node ($j \in N_l$) for choosing a higher transmission power level is a concave function.*

Proof: Let the current and the new transmission power levels of node $j \in N_l$ be p_j and $\tilde{p}_j$, respectively. The change in the power level is denoted by $\wp_j = \tilde{p}_j - p_j$. Transmission of a message using a higher transmission power requires higher transmission energy. Thus, the energy consumption of the localized nodes increases due to participation in 'opportunistic localization'.

Let the profit achieved for message transmission using power level p_j and $\tilde{p}_j$ be given by $\mathcal{P}_j(p_j)$, and $\mathcal{P}_j(\tilde{p}_j)$, respectively. Therefore, $\mathcal{P}_j(p_j) \geq \mathcal{P}_j(\tilde{p}_j)$, as $p_j \leq \tilde{p}_j$.

Thus, the rate of change of profit with respect to the transmission power level variation is non-increasing. So,

$$\frac{d\mathcal{P}_j}{d\wp_j} \leq 0 \tag{16}$$

Hence, $\mathcal{P}_j(\cdot)$ is a concave function. □

4.2.2 Utility function for Unlocalized Nodes

In the Stackelberg game of localization, the unlocalized nodes are the leaders. They watch for the decision of the localized nodes, and based on the response of the followers, they maximize their profits. The strategy of the leader is to minimize the energy consumption during localization delay. We define the rules for calculating the utility Ψ_i for any leader i as follows.

The utility of any leader i for follower j increases with the decrease in localization delay. Let t_{ij} denote the two-round trip time of messages between the follower j and leader i. The follower waits for $n_{ref}|_{max}$ number of location beacons before starting the localization process. Also, the utility of the leader i decreases with each retry it does to send the OReq message. As with each such retry, the leader has to transmit again using power level p_i. Therefore, for any fixed power level p_j of the follower j,

$$\Psi_i = \sum_{\substack{j \in N_l, \\ |j| \leq n_{ref}|_{max}}} \Psi_{ij}$$

$$\text{or, } \Psi_i = p_i \sum_{\substack{j \in N_l, \\ |j| \leq n_{ref}|_{max}}} t_{ij} \tag{17}$$

where $p_{min} < p_j \leq p_{max}$.

4.2.3 Existence of the Stackelberg-Nash-Cournot Equilibrium

The game reaches the equilibrium, when the leader or the unlocalized node minimizes its localization delay, and the localized nodes (the followers) reach their equilibrium state. In such a state, the players cannot improve their individual profit by single-sidedly changing their actions. The Stackelberg-Nash-Cournot Equilibrium of the Single-Leader-Multi-Follower Stackelberg game $\mathcal{G} = \langle \{N_l \cup N_{ul}\}, P(t), W(t), \{\Psi_l\}_{l \in N_{ul}}, \{\mathcal{U}_f\}_{f \in N_l} \rangle$ exists for the selection of optimal power level (p_j^*) by the follower j, if the following inequality is satisfied.

$$\mathcal{U}_j(p_j^*, \mathbf{p}_{-j}^*) \geq \mathcal{U}_j(\tilde{p}_j, \mathbf{p}_{-j}^*) \tag{18}$$

where $\mathbf{p}_{-j}^* = (p_1^*, p_2^*, \cdots, p_{j-1}^*, p_{j+1}^*, \cdots, p_n^*)$.

Theorem 3. *The localized nodes maximize their transmission power to maximize their individual profits by localizing more nodes. Therefore, the localized nodes reach to Stackelberg-Nash-Cournot Equilibrium by maximizing the transmission power to a certain level, i.e., power at the equilibrium level p_j^*, when the following condition holds:*

$$\frac{\Delta U_j}{\Delta \tilde{p}_j} = \frac{U_j(\tilde{p}_j + \delta p_j) - U_j(\tilde{p}_j)}{(\tilde{p}_j + \delta p_j) - \tilde{p}_j} \geq 0$$

where $p_j^* = \tilde{p}_j + \delta p_j$.

Proof:

$$\frac{\Delta U_j}{\Delta \tilde{p}_j} = \frac{U_j(\tilde{p}_j + \delta p_j) - U_j(\tilde{p}_j)}{(\tilde{p}_j + \delta p_j) - \tilde{p}_j}$$

This article has been accepted for publication in a future issue of this journal, but has not been fully edited. Content may change prior to final publication. Citation information: DOI 10.1109/TMC.2014.2338293, IEEE Transactions on Mobile Computing

$$= \left\{\frac{1}{\delta p_j}\right\}\Big[\Big\{tan^{-1}(e^{-\frac{\Delta p_j+\delta p_j}{p_j}}) + n_{OReq}^{(\tilde{p}_j+\delta p_j)}(\tilde{p}_j+\delta p_j) \left(\frac{1}{n_{OReq}} + \frac{1}{\sum_{k=1}^{n_{OReq}} n_{ref}^k}\right)\Big\} - \Big\{tan^{-1}\left(e^{-\frac{\Delta p_j}{p_j}}\right) + n_{OReq}^{\tilde{p}_j}\tilde{p}_j\left(\frac{1}{n_{OReq}} + \frac{1}{\sum_{k=1}^{n_{OReq}} n_{ref}^k}\right)\Big\}\Big]$$

$$= \left\{\frac{1}{\delta p_j}\right\} \Big[\left\{tan^{-1}\left(e^{-\frac{\Delta p_j+\delta p_j}{p_j}}\right) + n_{OReq}^{(\tilde{p}_j+\delta p_j)}\left(\tilde{p}_j+\delta p_j\right)\mathcal{K}\right\} - \left\{tan^{-1}\left(e^{-\frac{\Delta p_j}{p_j}}\right) + n_{OReq}^{\tilde{p}_j}\tilde{p}_j\mathcal{K}\right\}\Big] \quad (19)$$

where $\mathcal{K} = \left(\frac{1}{n_{OReq}} + \frac{1}{\sum_{k=1}^{n_{OReq}} n_{ref}^k}\right)$.

Here, we have to prove that the first term $\{\cdot\} \geq 0$ and $[\cdot] \geq 0$

$$\left\{tan^{-1}\left(e^{-\frac{\Delta p_j+\delta p_j}{p_j}}\right) + n_{OReq}^{(\tilde{p}_j+\delta p_j)}\left(\tilde{p}_j+\delta p_j\right)\mathcal{K}\right\} - \left\{tan^{-1}\left(e^{-\frac{\Delta p_j}{p_j}}\right) + n_{OReq}^{\tilde{p}_j}\tilde{p}_j\mathcal{K}\right\}$$

$$= \left\{tan^{-1}\left(e^{-\frac{\Delta p_j+\delta p_j}{p_j}}\right) - tan^{-1}\left(e^{-\frac{\Delta p_j}{p_j}}\right)\right\} + \left\{2 \times n_{OReq}^{\tilde{p}_j+\delta p_j}\tilde{p}_j - n_{OReq}^{\tilde{p}_j}\tilde{p}_j\right\}\mathcal{K} \quad (20)$$

The second term $\{\cdot\} \geq 0$, as $n_{OReq}^{(\tilde{p}_j+\delta p_j)} \geq n_{OReq}^{\tilde{p}_j}$. Also, $\delta p_j \geq 0$, as $\Delta p_j + \delta p_j \geq \Delta p_j$ and $n_{OReq}^{\tilde{p}_j+\delta p_j} > 0$. Now,

$$tan^{-1}\left(e^{-\frac{\Delta p_j+\delta p_j}{p_j}}\right) - tan^{-1}\left(e^{-\frac{\Delta p_j}{p_j}}\right) = tan^{-1}\left(\frac{e^{-\frac{\Delta p_j+\delta p_j}{p_j}} - e^{-\frac{\Delta p_j}{p_j}}}{1 + e^{-\frac{\Delta p_j+\delta p_j}{p_j}} e^{-\frac{\Delta p_j}{p_j}}}\right) = tan^{-1}\left(\frac{e^{-\frac{\Delta p_j+\delta p_j}{p_j}} - e^{-\frac{\Delta p_j}{p_j}}}{1 + e^{-\frac{2\Delta p_j+\delta p_j}{p_j}}}\right)$$

.

Hence, if $(\cdot) \geq 0$, the Theorem can be proved. Therefore,

$$\frac{e^{-\frac{\Delta p_j+\delta p_j}{p_j}} - e^{-\frac{\Delta p_j}{p_j}}}{1 + e^{-\frac{2\Delta p_j+\delta p_j}{p_j}}} = \frac{e^{-\frac{\Delta p_j}{p_j}}\left[e^{-\frac{\delta p_j}{p_j}} - 1\right]}{1 + e^{-\frac{2\Delta p_j+\delta p_j}{p_j}}} \quad (21)$$

From the Equation 21, we get,

$$e^{-\frac{\delta p_j}{p_j}} - 1 \geq 0$$

as $\delta p_j \geq 0$, and $1 + e^{-\frac{2\Delta p_j+\delta p_j}{p_j}} \geq 1$.

Hence, $\frac{\Delta U_j}{\Delta \tilde{p}_j} \geq 0$, which proves the Theorem. □

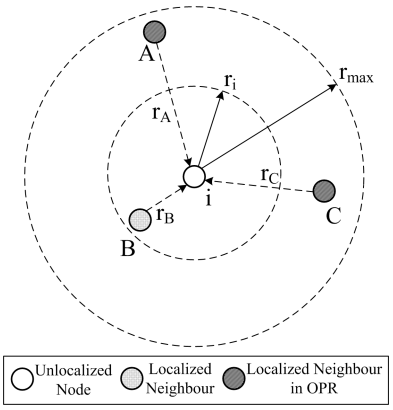

Fig. 2: A scenario depicting the necessity of opportunistic localization

4.3 Opportunistic Localization

The nodes deployed over the surface of water act as the initial anchor nodes for the unlocalized nodes. The localization process is anchor-initiated. The anchors broadcast 'Wakeup' message at power p_j to inform the unlocalized nodes about its presence. Any unlocalized node is able to localize itself after receiving the required number of beacon messages ($n_{ref}|_{max}$) from different anchor nodes. This is the required criterion for localization. However, in sparse UWSNs, such condition is not always fulfilled. Therefore, the nodes explore their available opportunities by increasing the transmission range. The unlocalized nodes broadcast the 'OReq' message at power p_{max} to find its 'Maximum Opportunistic Region' ($\mathbf{MaxOPR_i}|_{i \in N_{ul}}$). After receiving the 'OReq' messages, a localized node decides its optimal transmission power level ($\tilde{p}_j$), to maximize its profit. The unlocalized nodes again execute their localization procedure after receiving the required number of messages from its localized neighbors.

Figure 2 depicts a scenario consisting of one leader i and three followers, A, B, and C. Initially, the unlocalized leader has only one neighbor B in its range. However, when it starts opportunistic localization by transmitting at p_{max} power to have a transmission radius of r_{max}, it finds three localized nodes. The followers, on the other hand, select their optimal power levels $\{\tilde{p}_j\}_{j \in A,B,C}$, based on the received requests from the leaders. Accordingly, the selected transmission ranges are r_A, r_B, and r_C, as in our example in Figure 2.

In this scheme, the existing localized nodes have the objective to help localize maximum number of nodes with minimum energy consumption. Mathematically,

$$\max_{j \in N_l} \mathcal{U}_j = \tan^{-1}(e^{-\frac{\tilde{p}_j - p_j}{p_j}}) + \left(\frac{n_{OReq}^{\tilde{p}_j}}{n_{OReq}} + \frac{n_{OReq}^{\tilde{p}_j}}{\sum_{k=1}^{n_{OReq}} n_{ref}^k}\right)\tilde{p}_j \quad (22)$$

On the other hand, the objective of the unlocalized nodes is to minimize the localization delay. An unlocalized node waits for $n_{ref}|_{max}$ number of location beacons

This article has been accepted for publication in a future issue of this journal, but has not been fully edited. Content may change prior to final publication. Citation information: DOI 10.1109/TMC.2014.2338293, IEEE Transactions on Mobile Computing

to be successfully localized. Mathematically,

$$\min_{i \in N_{ul}} \Psi_i = p_i \sum_{\substack{j \in N_l, \\ |j| \leq n_{ref}|_{max}}} t_{ij} \quad (23)$$

4.3.1 Algorithm for Unlocalized Nodes

To start opportunistic localization, the unlocalized nodes first explore their *maximum opportunities* by following the procedure described in Algorithm 1. An unlocalized node broadcasts a packet named 'Opportunity Request' or 'OReq', to explore its $\mathbf{MaxOPR_i}$. Any unlocalized node is able to localize itself after finding the total number of required reference nodes ($n_{ref}|_{max}$), which is the sum of the *opportunistic reference nodes* and the available reference nodes. The number of available reference nodes is found by counting the number of 'Wakeup' messages received.

Algorithm 1 Algorithm for Unlocalized Nodes

Inputs: N_{ul}, N_l, $\{Nbr(i)\}_{p_i; i \in N_{ul}}$, $\{W_i(t)\}_{i \in N_{ul}}$, $P(t)$.
Output: Localization delay t_{delay}.

1: **for** each 'Wakeup' message received from a localized node $j \in \{Nbr(i)\}_{p_i; i \in N_{ul}}$ **do**
2: Add j to $\{J\}_{p_i}$.
3: **end for**
4: **if** $|\{J\}_{p_i}| \geq 0$ **then**
5: $n^i_{ref} \longleftarrow (n_{ref}|_{max} - |\{J\}_{p_i}|)$.
6: **else**
7: $n^i_{ref} \longleftarrow n_{ref}|_{max}$.
8: **end if**
9: **if** $W_i(t) > W_{th}$ **then**
10: Send 'OReq' message at power $p_i \longleftarrow p_{max}$.
11: **else**
12: Remaining energy LOW, do not transmit 'OReq'.
13: **end if**
14: **for** 'ORply' message received from node j **do**
15: Calculate $d_{ij} \longleftarrow (t_i - t_j) \times v_{sound}$.
16: **if** Number of beacons received = $n_{ref}|_{max}$ **then**
17: Localize().
18: Return $t_{delay} \longleftarrow t_{now} - t_{init}$.
19: **end if**
20: **end for**

Theorem 4. *An unlocalized node $i \in N_{ul}$ always starts opportunistic localization by transmitting the 'OReq' message using power $p_i = p_{max}$, if it satisfies $W_i(t) > W_{th}$ at time t.*

Proof: The goal of an unlocalized node ($i \in N_{ul}$) is to localize by minimizing the localization delay (t_{loc}).

$$\min_{i \in N_{ul}} t_{loc} = \sum_{\substack{j \in N_l, \\ |j| \leq n_{ref}|_{max}}} t_{ij} \quad (24)$$

According to Theorem 4.2.1 and Definition 1, the $\mathbf{OPR_S}$ of an unlocalized node S have higher number of localized nodes, which act as potential anchors for the unlocalized node to get localized. Let S have three different transmission power levels p_i, $\bar{p}_i$, p_{max} and let the corresponding transmission ranges be r_i, $\bar{r}_i$, r_{max}, respectively. Here, $p_i < \bar{p}_i < p_{max}$ and $r_i < \bar{r}_i < r_{max}$.

Let n_k represent the number of localized neighbors present in the transmission range $k \in \{r_i, \bar{r}_i, r_{max}\}$. Then, we consider the probability of *not finding* any localized node as the following.

$$Prob(n_k < 1) = \begin{cases} \alpha & \text{for } k = r_i, \\ \beta & \text{for } k = \bar{r}_i, \\ \gamma & \text{for } k = r_{max} \end{cases} \quad (25)$$

where it is straightforward to verify that $\alpha \geq \beta$ and $\beta \geq \gamma$. Thus, considering $Prob(n_k \geq 1) = 1 - Prob(n_k < 1)$, the probability to find at least one localized node is,

$$Prob(n_k \geq 1) = \begin{cases} 1-\alpha & \text{for } k = r_i, \\ 1-\beta & \text{for } k = \bar{r}_i, \\ 1-\gamma & \text{for } k = r_{max} \end{cases} \quad (26)$$

Consequently, we can derive,

$$\begin{aligned} Prob(n_{\bar{r}_i} \geq 1) - Prob(n_{r_i} \geq 1) &= (1-\beta) - (1-\alpha) \\ &= \alpha - \beta \ [\because \alpha \geq \beta] \\ &> 0 \end{aligned} \quad (27)$$

Hence, $Prob(n_{\bar{r}_i} \geq 1) \geq Prob(n_{r_i} \geq 1)$ and similarly, $Prob(n_{r_{max}} \geq 1) \geq Prob(n_{\bar{r}_i} \geq 1)$.

Thus, the probability to find a localized neighbor is non-decreasing with the transmission range. Mathematically,

$$Prob(n_{r_{max}} \geq 1) \geq Prob(n_{\bar{r}_i} \geq 1) \geq Prob(n_{r_i} \geq 1) \quad (28)$$

Hence, an unlocalized node S always explores $\mathbf{MaxOPR_S}$ to ensure finding maximum number of localized nodes. Thus, $p_i = p_{max}$ for $W_i(t) > W_{th}$. Otherwise, the localization delay and energy consumption increases due to repeated retry attempts. □

Corollary 1. *The unlocalized nodes (N_{ul}) do not collude among themselves.*

Proof: Let two unlocalized nodes S_1 and S_2 collude among themselves, and choose to reduce their individual transmission range (r_1, r_2), such that $r_1, r_2 < r_{max}$.

Therefore, according to Theorem 4, the probability to reach potential anchors for both S_1 and S_2 is less than their maximum opportunities. Also, any retry by S_1 and S_2 will increase the localization delay for each of them.

We consider that the prioritized goal of any unlocalized node $S_1, S_2 \in N_{ul}$ is to get localized while minimizing t_{loc} to maximize their individual profit, when the remaining battery power is higher than the threshold level ($W_i(t) > W_{th}$).

Hence, no unlocalized node colludes among themselves. □

This article has been accepted for publication in a future issue of this journal, but has not been fully edited. Content may change prior to final publication. Citation information: DOI 10.1109/TMC.2014.2338293, IEEE Transactions on Mobile Computing

4.3.2 Algorithm for Localized Nodes

The procedure followed by a localized node or an anchor is described in Algorithm 2. Initially, 'Wakeup' messages are broadcasted by the anchor nodes to inform the unlocalized nodes about their presence. Any follower calculates the required transmission power level, and its corresponding utility. Thereafter, an optimized transmission power level (p_i) is taken, based on the strategy abstracted in Equation 22. During all these transmissions, the battery status of a node is taken into consideration. For low residual battery power, i.e., $W_j(t) \leq W_{th}$, a node is debarred from any transmission.

Algorithm 2 Algorithm for Localized Nodes

Inputs: N_l, N_{ul}, $\{W_j(t)\}_{j \in N_l}$, $P(t)$.
Output: Optimized action $\tilde{p}_j$.

1: **if** $W_j(t) > W_{th}$ **then**
2: Broadcast 'Wakeup' message at power p_i.
3: **else**
4: Remaining energy LOW, do not transmit.
5: **end if**
6: **for** 'OReq' packet received from node $i \in N_{ul}$ **do**
7: Calculate $d_{ji} \longleftarrow (t_j - t_i)v_{sound}$.
8: Calculate required transmission power $\tilde{p}_j$.
9: Get n^i_{ref}.
10: Calculate utility $\mathcal{U}_j$.
11: **end for**
12: Compute $n_{_{OReq}}$.
13: **if** $n_{_{OReq}} > 0$ **then**
14: **if** $W_j(t) > W_{th}$ **then**
15: Return $\tilde{p}_j \longleftarrow \arg\max_{j \in N_l} \mathcal{U}_j$.
16: Broadcast $ORply$ at power $\tilde{p}_j$.
17: **else**
18: Remaining energy LOW; do not transmit.
19: **end if**
20: **end if**

Lemma 2. *The decision of a localized node is based on zero conjecture variation, i.e., other localized nodes will hold their strategies as in the existing level.*

Proof: Let the profit for any follower $j \in N_l$ may be represented by

$$\mathcal{P}_j(p_j) \propto n^{p_j}_{OReq}$$
$$\mathcal{P}_j(p_j) = k_j \times n^{p_j}_{OReq} \tag{29}$$

Let at any time t, the strategies of the followers be $P = \{p_1, p_2, \ldots, p_j, \ldots, p_{|N_l|}\}$, and the corresponding profits are, $\mathcal{P} = \{n_1, n_2, \ldots, n_j, \ldots, n_{|N_l|}\}$, where $n_j = k_j \times n^{p_j}_{OReq}$.

Assume that follower j changes its strategy from p_j to $\bar{p}_j$, and the corresponding profit changes as,

$$\bar{\mathcal{P}} = \{n_1, n_2, \ldots, \bar{n}_j, \ldots, n_{|N_l|}\} \tag{30}$$

Therefore, the change in profits is,

$$\bar{\mathcal{P}} \sim \mathcal{P} = \{0, 0, \ldots, \bar{n}_j \sim n_j, \ldots, 0\} \tag{31}$$

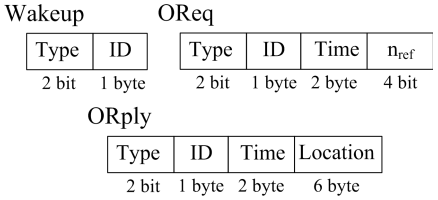

Fig. 3: Message formats used in OLTC

Then, the *conjecture variation*, δ_j, is calculated as the ratio of the combined output variation of the followers, $\forall i \in N_l$ and $i \neq j$, to the j^{th} follower,

$$\delta_j = \frac{d(\sum_{i \neq j} p_i)}{dp_j} \tag{32}$$

Therefore,

$$\delta_j = \frac{d(\sum_{i \neq j} p_i)}{dp_j} = \frac{0}{\bar{n}_j \sim n_j} = 0 \tag{33}$$

This concludes the proof. □

4.3.3 Message Formats

In OLTC, three types of messages are used – *Wakeup*, *Opportunity Request* (*OReq*), and *Opportunity Reply* (*ORply*). 'Wakeup' message is broadcast to initiate the scheme. Thereafter, 'OReq' is broadcast on-demand by the unlocalized nodes, if they lack the required number of beacons. In reply to 'OReq', the 'ORply' message is broadcast by the localized nodes after selecting an optimal transmission power level. The location information of the reference (localized) nodes is embedded in the 'ORply' message. Therefore, the 'ORply' message acts as a location beacon as well. These message formats are shown in Figure 3. In each message, the message type and sender node's id is embedded. Additionally, 'OReq' includes the time of message send from the unlocalized node, and the required number of reference nodes. In 'ORply', the node's location information is included in addition to the sending time information.

5 Results and Discussions

5.1 Simulation Settings

We simulated the proposed scheme using the NS-3 (http://www.nsnam.org/) simulation platform. We varied the number of nodes from 10-50 in the deployment region of 2500 $m\times$ 2500 $m\times$ 2500 m. This provides us to experiment on low to medium node density scenarios. For each scenario we deployed four anchor nodes on the water surface. Each simulation was executed for 100 $seconds$. Initially, the transmission range of the nodes was set to 1000 m. We considered $R_i = [1000\ m, 1500\ m, 2000\ m]$, where the number of different transmission power levels $\kappa = 3$. In the simulations, we set the transmission power level p_i (`TxPower` (in dB) attribute in `UanPhyGen` model) for a given range

This article has been accepted for publication in a future issue of this journal, but has not been fully edited. Content may change prior to final publication. Citation information: DOI 10.1109/TMC.2014.2338293, IEEE Transactions on Mobile Computing

TABLE 2: Simulation Parameters

Parameter	Value
Transmission Range (r)	1000-2000 m
Node mobility (v_m)	0.5-2.0 m/s
Node mobility model	Meandering Current Mobility model [32]
Channel frequency	22 KHz
Modulation technique	FSK
Data rate	500 bps
Speed of sound	1500 m/s
Wave propagation model	Thorp's propagation model [31]
Transmission power	0.203 $watts$ [33]
Receive & Idle power	0.024 $watts$ [33]
Sleep power	3×10^{-6} $watts$ [33]
Initial energy of a node	200 J
Threshold battery level (W_{th})	50 J

(r_i) as the propagation loss incurred for that particular transmission range using the Thorp's propagation model [31]. Other simulation parameters are listed in Table 2.

In each simulation, the nodes are initially placed randomly inside the simulation region boundary. Thereafter, they move according to the velocity of ocean current, by following the Meandering Current Mobility model [32]. The process of node localization is distributed throughout the network. Any unlocalized node gets localized after receiving $n_{ref}|_{max}$ number of beacons from its one-hop neighbors, which are already localized. We use the trilateration technique for node localization, and thus, we consider $n_{ref}|_{max} = 3$. Any node acts as a *reference node* to its *one-hop* neighbors only. Thus, the initial simulation boundary does not have any effect on the localization process.

5.2 Performance Metrics

We evaluated the performance of the proposed algorithm using the following metrics:

(i) *Localization coverage:* It is defined as the ratio of the number of localized nodes to the total number of nodes in the network.

(ii) *Average energy consumption per node:* It is measured as the ratio of the total energy consumption to the number of localized nodes. Average energy consumption is calculated as, $\mathcal{E}_{avg} = \frac{1}{N}\sum_{i=1}^{N}\mathcal{E}_i$.

(iii) *Average localization error:* Average localization error is calculated using the following formula: $\epsilon = \frac{1}{N}\sum_{i=1}^{N}\sqrt{(x_i - x_i')^2 + (y_i - y_i')^2 + (z_i - z_i')^2}$, where for any node i, (x_i,y_i,z_i) and (x_i',y_i',z_i') denote the estimated, and the original locations, respectively.

(iv) *Average localization delay:* It is measured as the average time to localize a node after it receives the 'Wakeup' message.

5.3 Benchmark

We compared the performance of OLTC with two well-known localization schemes, namely, the Three Dimensional Localization Algorithm for Underwater Acoustic Sensor Networks (3DUL) [12], and the Dive'N'Rise Localization (DNRL) [16], for UWSNs. Both 3DUL and DNRL, were simulated with setting the transmission range of the sensor nodes at $r_i = r_{max} = 1000\ m$, and $r_i = r_{max} = 2000\ m$. 3DUL is an surface anchor initiated iterative 3-dimensional localization scheme, whereas DNRL incorporates special type of mobile agents, called the DNR beacons, to aid the node localization procedure. In the simulations, the transmission range of the sensor nodes (in 3DUL) and the DNR beacons (in DNRL) was set to 1000 m for both the schemes. For the simulation of DNRL, we placed DNR beacons, which dive and rise along the depth of the water column maintaining a constant velocity of 2.5 m/s (4.86 $Knot$). These DNR beacons were deployed randomly throughout the simulation region, and they broadcasted their coordinates periodically. We assumed that the DNR beacons drifted horizontally due to the effect of underwater currents.

TABLE 3: Inter-node distance

No. of Nodes	Inter-node Distance		
	Avg.	Min.	Max.
10	1641.4746	1588.0529	1694.8962
20	1652.598	1621.2923	1683.9036
30	1644.855	1619.5548	1670.1551
40	1646.1324	1622.9186	1669.3461
50	1648.6572	1627.9064	1669.4079

In addition to 3DUL and DNRL, we also simulated another scheme similar to OLTC, however, without any topology control, i.e., the nodes did not change the transmission range 'opportunistically'. We named this scheme as OLwoTC, where 'wo' signifies the fact that the scheme is *without* topology control. OLwoTC was simulated for two different transmission ranges of the sensor nodes — first case with $r_i = r_{max} = 1000\ m$, and second case with $r_i = r_{max} = 2000\ m$. Similar to OLTC, in OLwoTC as well, we placed four anchor nodes on the water surface to initiate the localization process. Other simulation parameters remained the same as described in Table 2.

Justification for the Selection of Transmission Range: Table 3 shows the initial inter-node distance for node deployments consisting of 10-50 nodes in a 2500 $m\times$ 2500 $m\times$ 2500 m region. Statistically, the results are computed with 95% confidence. The inter-node distance decreases marginally with the increase in node density. Such node distribution motivates the selection of choosing the transmission range $R_i = [1000\ m, 1500\ m, 2000\ m]$. Similarly, we simulated the benchmark schemes using the minimum ($r_i = 1000\ m$) and the maximum ($r_i = 2000\ m$) transmission ranges.

Additionally, underwater acoustic modems with long transmission range in the order of few kilometers are available commercially. For example, the Teledyne modems 865-A and ATM-886 have transmission range up to 10 km (http://www.teledynemarine.com/flash/index.html).

This article has been accepted for publication in a future issue of this journal, but has not been fully edited. Content may change prior to final publication. Citation information: DOI 10.1109/TMC.2014.2338293, IEEE Transactions on Mobile Computing

5.4 Results and Analysis

5.4.1 Localization coverage

We measured the number of successfully localized sensor nodes for OLTC and the benchmark schemes — 3DUL, DNRL, and OLwoTC. In this experiment, we varied the number of deployed nodes between 10 to 50, and set the node mobility (v_m) to 0.5 m/s. Both 3DUL and DNRL, when simulated with $r_i = r_{max} = 1000\ m$, attain very low number of successfully localized nodes compared to OLTC. In this settings, compared to OLTC, the localization coverage achieved in 3DUL and DNRL is respectively 23.92% and 35.59% lower, on an average. However, in case of $r_i = r_{max} = 2000\ m$, OLTC results in nearly 21.94% and 18.92% lower localization success compared to 3DUL and DNRL, respectively. As proved in Theorem 4.2.1, an increased transmission range results in increased *ability* of a node to localize other nodes. In OLTC, an existing localized node dynamically selects a transmission range so as to maximize the number of neighbors yet to be localized. Hence, OLTC has a better chance of success than 3DUL and DNRL for $r_i = 1000\ m$, and less chance than 3DUL and DNRL for $r_i = 2000\ m$. The localization coverage achieved using 3DUL scheme nearly follows the same as that achieved for the scheme where topology control is not used (OLwoTC, range at 1000 m). This is because of the similar type of protocol design incorporated in both the schemes. On the other hand, in case of DNRL, the localization coverage is lower than that corresponding to 3DUL. In both the cases, the number of successfully localized nodes gradually increases with the increase in deployed node density. However, the rate of such increase in higher in case of 3DUL than in DNRL.

We also compared the localization coverage in OLTC with OLwoTC by varying the transmission range between 1000 m and 2000 m. The results of this experiment are shown in Figure 4. The localization coverage achieved in OLTC is nearly 17.65% higher than OLwoTC, when the transmission range is 1000 m. However, the localization coverage achieved in OLwoTC is nearly 23.51% lower in OLTC, when the transmission range increases to 2000 m. Therefore, using a fixed transmission range of 2000 m in OLwoTC, rather than dynamically selecting it from a range of [1000 m, 1500 m, 2000 m], as in OLTC, the localization coverage increases. In OLTC, the localized nodes select a transmission range in such a fashion that maximum number of localized nodes are served with reduced energy consumption. Due to this, the selected transmission range in OLTC is sometimes less than 2000 m. Consequently, the localization coverage results in lower number of localized nodes than that in the case of $r_i = 2000\ m$. However, the increased localization coverage of OLwoTC (with 2000 m transmission range) costs higher energy consumption, which is discussed in Section 5.4.2.

We calculate the localization coverage for different scenarios consisting of different number of nodes, and

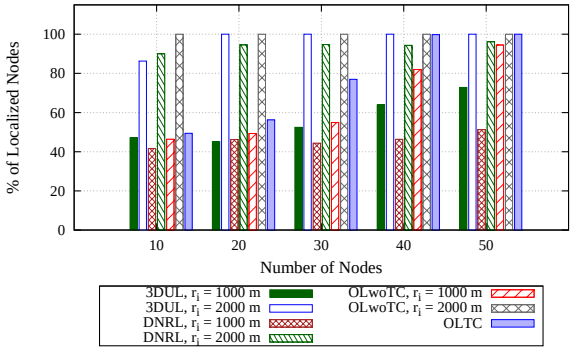

Fig. 4: Localization Coverage ($v_m = 0.5\ m/s$)

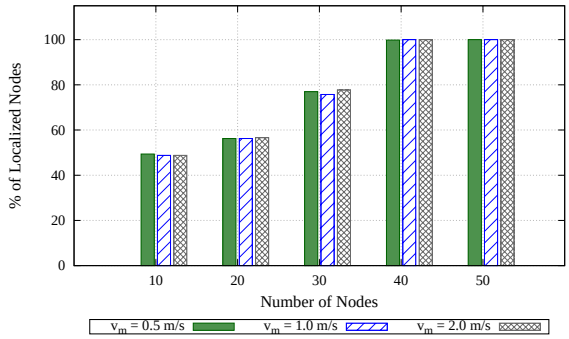

Fig. 5: Localization Coverage in OLTC

$v_m = 0.5, 1.0, 2.0\ m/s$. The results are plotted in Figure 5. From the results, we notice that with the increase in the number of deployed nodes, the localization coverage, i.e., the number of localized nodes in the network, increases. This observation is attributed to the node density factor. The increase in the node density helps in attaining higher localization coverage. The localization coverage mostly increases with the increase in the node mobility in the higher node density deployments.

5.4.2 Average energy consumption per localized node

The results of comparison for the metric, average energy consumption per localized node, is shown in Figure 6. We notice that the energy consumption of DNRL is the lowest among all the five schemes — OLTC, OLwoTC, 3DUL, and DNRL. It is noteworthy to mention that the energy consumption of the DNR beacons are excluded in the computation. However, OLTC depicts second-best order in energy-efficiency. Compared to 3DUL and OLwoTC with $r_i = 1000\ m$, the energy consumption per localized node is, respectively, 91.2% and 83.3% lower in OLTC. Although, in these schemes, the transmission range is comparatively lower — fixed to 1000 m, rather than dynamic in the range of 1000-2000 m. The lower localization success of the nodes continues to ignite the repeated try, which indeed is the reason for such behavior. Also, compared to OLwoTC, when the transmission range is set to 2000 m, energy consumption is nearly 91.82% lower in OLTC. In this case, the relative difference of the localization success is nearly 23.51%

This article has been accepted for publication in a future issue of this journal, but has not been fully edited. Content may change prior to final publication. Citation information: DOI 10.1109/TMC.2014.2338293, IEEE Transactions on Mobile Computing

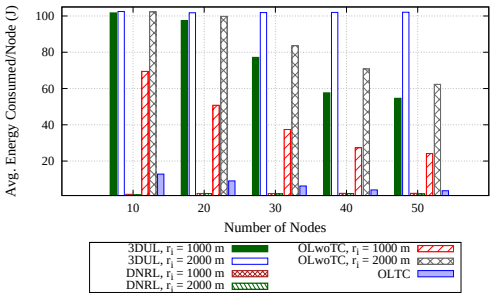

Fig. 6: Average Energy Consumption per Localized Node ($v_m = 0.5\ m/s$)

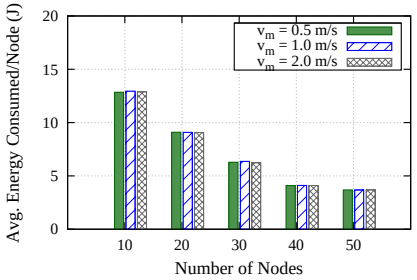

Fig. 7: Average Energy Consumption per Localized Node in OLTC

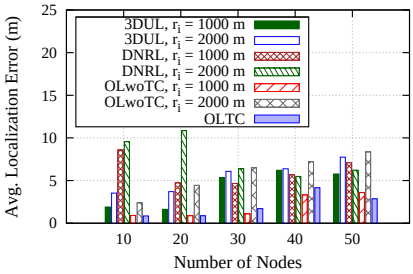

Fig. 8: Average Localization Error ($v_m = 0.5\ m/s$)

lower in OLTC. Thus, the use of higher transmission power results in higher energy consumption of nodes in OLwoTC. Compared to 3DUL with $r_i = 2000\ m$, OLTC results in 92.94% lesser average energy consumption per node. Thus, compared to 3DUL and OLwoTC, OLTC maintains energy-efficiency. This behavior is attributed to the design goal of the OLTC scheme — energy-efficient selection of transmission range. On the other hand, in 3DUL and OLwoTC, nodes do not perform any such trade-off. However, OLTC depicts increased energy consumption compared to DNRL. The average energy consumption per node is approximately 62.65% and 67.08% lower in DNRL for $r_i = 1000\ m$ and $r_i = 2000\ m$, respectively. In DNRL, the anchor nodes and the unlocalized sensor nodes exchange 'silent' messages, i.e., the unlocalized nodes only receive the beacon messages from the anchors. Thus, the energy consumption of the nodes is only due to receiving of messages, which helps to maintain a low energy consumption profile in DNRL. On the other hand, in OLTC, the dynamic use of topology control helps in attaining higher success rate of node localization, and comparatively lower overall energy consumption.

Figure 7 shows the results for the average energy consumption per localized node. It is observed that with increase in the number of deployed nodes, the average energy consumption per node decreases. It is because of the increase in the node density in the network that an anchor j has more number of unlocalized nodes present in its $\mathbf{OPR_j}$. Consequently, energy consumption value per node also decreases. With the variation in $v_m = 0.5, 1.0, 2.0\ m/s$, the variation in average energy consumption is not significant.

5.4.3 Average Localization Error

Figure 8 shows the results of comparison for average localization error induced during localization for OLTC, 3DUL, DNRL, and OLwoTC. In case of OLwoTC with transmission range 1000 m and 2000 m, the error value is nearly 4.75% lower and 2.25 times higher than OLTC, respectively. The higher is the node density, the higher is the average error for both these cases. The location estimation error occurring in 3DUL is 50.45% and 64.29% lower in OLTC for $r_i = 1000\ m$ and $r_i = 2000\ m$, respectively. The increase in average localization error is due to the increase in the transmission range. Compared to DNRL, the average localization error using OLTC is 64.32% and 66.85% lower, for $r_i = 1000\ m$ and $r_i = 2000\ m$, respectively. Similar to OLTC, in 3DUL and OLwoTC as well, the location estimation error increases with the increase in the node density in the deployment. However, it does not show the exactly similar trend in case of DNRL. The cause of such behavior can be explained following the mechanism of iterative location estimation. Except DNRL, all the other three schemes use iterative location estimation. In such schemes, the neighbors of the anchors are localized first, and then the neighbors of those nodes are localized, and the process continues. Therefore, in each iteration, the previous estimation error is induced in the current estimation. On the other hand, in DNRL, the nodes localize themselves by receiving the coordinates directly from the DNR beacons. However, in DNRL, the average localization error value is higher, which is mostly attributed to the mobile DNR beacons. Also, unlike the other schemes, with increase in the transmission range, the average localization error decreases in DNRL.

The average localization error in OLTC is plotted in Figure 9. The average error value increases with the increase in the deployment node density. This feature is attributed to the iterative nature of the scheme. For the low node density scenarios, the average localization error is also low. With lower node density, less number of nodes are present in the opportunistic region ($\mathbf{OPR_j}$) of an anchor j. Similarly, it is possible for more number of nodes to be localized by an anchor when the node density is higher. For this reason, the localization error increases in case of higher node density (such as 40-50 nodes). On the other hand, for low node density scenarios (such as 10-20 nodes), the change in average localization error is insignificant with the change in node mobility values.

This article has been accepted for publication in a future issue of this journal, but has not been fully edited. Content may change prior to final publication. Citation information: DOI 10.1109/TMC.2014.2338293, IEEE Transactions on Mobile Computing

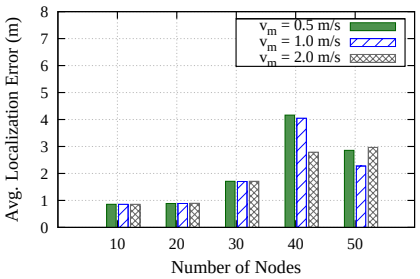

Fig. 9: Average Localization Error in OLTC

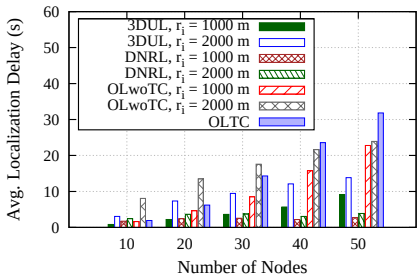

Fig. 10: Average Localization Delay ($v_m = 0.5\ m/s$)

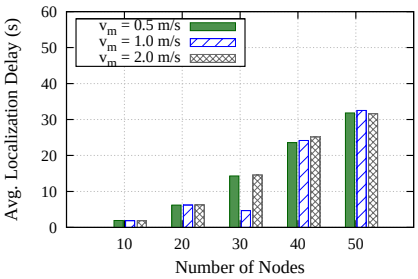

Fig. 11: Average Localization Delay in OLTC

5.4.4 Average Localization Delay

Figure 10 shows the results obtained for the metric localization delay in OLTC and the benchmark schemes. We find that by incorporating the topology control scheme, the localization delay increases in OLTC. Compared to OLTC, 3DUL results in reduced localization delay of nearly 68.8% and 12.23%, respectively, for $r_i = 1000\ m$ and $r_i = 2000\ m$. Also, in OLwoTC, the average localization delay is 28.71% lower and 85.87% higher compared to OLTC for $r_i = 1000\ m$ and $r_i = 2000\ m$, respectively. DNRL results in 66.98% and 52.47% less localization delay compared to OLTC. Such increase in the delay is caused due to longer distance travelled by the acoustic signal while the anchor nodes try to maximize their individual utility by increasing their transmission range to localize more number of sensor nodes. The average delay increases in all the schemes, except in DNRL, for increasing the number of deployed sensor nodes. For DNRL, the variation in average delay is very less throughout all the deployment scenarios. This is attributed to the uniform deployment of DNR-beacons throughout the simulation region.

Figure 11 shows the average localization delay with varying v_m. The results indicate the trend of increased node density with increased delay. In such a condition, more number of control messages are exchanged among the nodes. Due to this, on an average, the overall delay to localize a node, increases.

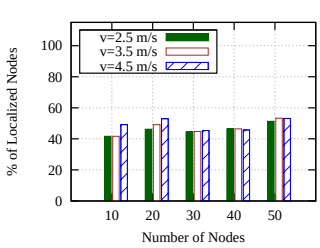

Fig. 12: Localization Coverage in DNRL

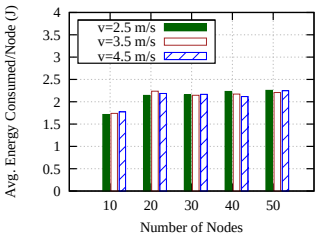

Fig. 13: Average Energy Consumption per Node in DNRL

5.4.5 DNR Velocity

We plot the localization coverage and average energy consumption per node with varying the DNR-beacon velocity (v) at 2.5, 3.5, and 4.5 m/s, in Figure 12 and 13, respectively. We observe that varying v from 2.5 m/s to 3.5 and 4.5 m/s, the localization coverage increases. However, the change in average energy consumption per localized node is marginal with the change in DNR-beacon velocity.

6 Conclusion

In this paper, we proposed a localization scheme named Opportunistic Localization by Topology Control (OLTC), specifically designed for sparse and partitioned UWSNs scenarios. In such scenarios, due to sparsity, most of the sensor nodes lack the presence of the required number of reference nodes to be able to localize. In OLTC, by exploiting topology control, such reference nodes are 'opportunistically' found and utilized. We formulate the scenario as a *Single-Leader-Multi-Follower Stackelberg game*, which describes an oligopoly among the unlocalized and the localized nodes. In the game model, an unlocalized node is considered as the *Stackelberg leader*, and an already localized node is described as the *Cournot follower*. Simulation results demonstrated that OLTC achieves nearly 76% localization coverage by spending nearly 3.6% battery power of any node. In case of $r_i = 1000\ m$, compared to the 3DUL and DNRL, OLTC achieves nearly 34.01% and 64.73% increased localization coverage. Compared to the 3DUL and DNRL simulated with $r_i = r_{max} = 2000\ m$, OLTC results in nearly 21.94% and 18.92% low localization coverage. However, for average energy consumption per node, OLTC is nearly 91.2% energy-efficient than 3DUL, even though, DNRL is more energy-efficient than OLTC.

In the future works, the proposed scheme may be modified to work in the presence of extreme UWSN challenging environments involving the presence of shadow zones, jamming, and natural interference. Also, in future, 'mixed strategy' for the nodes may be considered for selecting the appropriate transmission power level.

References

[1] J. Aspnes, T. Eren, D. K. Goldenberg, A. S. Morse, W. Whiteley, Y. R. Yang, B. D. Anderson, and P. N. Belhumeur, "A theory of network localization," *IEEE Trans. on Mobile Computing*, vol. 5, no. 12, pp. 1663–1678, 2006.

This article has been accepted for publication in a future issue of this journal, but has not been fully edited. Content may change prior to final publication. Citation information: DOI 10.1109/TMC.2014.2338293, IEEE Transactions on Mobile Computing

[2] M. Erol-Kantarci, H. T. Mouftah, and S. Oktug, "A survey of architectures and localization techniques for underwater acoustic sensor networks," *IEEE Communications Surveys and Tutorials*, vol. 13, no. 3, pp. 487–502, 2011.

[3] H.-P. Tan, R. Diamant, W. K. G. Seah, and M. Waldmeyer, "A survey of techniques and challenges in underwater localization," *Ocean Engineering*, vol. 38, no. 14, pp. 1663–1676, 2011.

[4] H. Chenji and R. Stoleru, "Toward accurate mobile sensor network localization in noisy environments," *IEEE Trans. on Mobile Computing*, vol. 12, no. 6, pp. 1094–1106, 2013.

[5] G. Isbitiren and O. B. Akan, "Three-dimensional underwater target tracking with acoustic sensor networks," *IEEE Trans. on Vehicular Technology*, vol. 60, no. 8, pp. 3897–3906, October 2011.

[6] S. Misra and S. Singh, "Localized policy-based target tracking using wireless sensor networks," *ACM Trans. on Sensor Networks*, vol. 8, no. 3, p. 27, 2012.

[7] P. Xie, J.-H. Cui, and L. Lao, "VBF: vector-based forwarding protocol for underwater sensor networks," in *Proc. of IFIP Networking*, 2006, pp. 1216–1221.

[8] I. F. Akyildiz, D. Pompili, and T. Melodia, "Underwater acoustic sensor networks: Research challenges," *Ad Hoc Networks*, vol. 3, no. 3, pp. 257–279, 2005.

[9] J. Partan, J. Kurose, and B. N. Levine, "A survey of practical issues in underwater networks," *ACM SIGMOBILE Mobile Computing and Communications Review*, vol. 11, no. 4, pp. 23–33, 2007.

[10] L. Liu, S. Zhou, and J.-H. Cui, "Prospects and problems of wireless communication for underwater sensor networks," *Wireless Communications and Mobile Computing*, vol. 8, no. 8, pp. 977–994, 2008.

[11] J. Heidemann, M. Stojanovic, and M. Zorzi, "Underwater sensor networks: applications, advances and challenges," *Philosophical Trans. of the Royal Society A*, vol. 370, pp. 158–175, 2012.

[12] M. T. Isik and O. B. Akan, "A three dimensional localization algorithm for underwater acoustic sensor networks," *IEEE Trans. on Wireless Communications*, vol. 8, no. 9, pp. 4457–4463, 2009.

[13] Z. Zhou, Z. Peng, J.-H. Cui, Z. Shi, and A. C. Bagtzoglou, "Scalable localization with mobility prediction for underwater sensor networks," *IEEE Trans. on Mobile Computing*, vol. 10, no. 3, pp. 335–348, 2011.

[14] X. Cheng, H. Shu, Q. Liang, and D. H.-C. Du, "Silent positioning in underwater acoustic sensor networks," *IEEE Trans. on Vehicular Technology*, vol. 57, no. 3, pp. 1756–1766, 2008.

[15] A. Y. Teymorian, W. Cheng, L. Ma, X. Cheng, X. Lu, and Z. Lu, "3D underwater sensor network localization," *IEEE Trans. on Mobile Computing*, vol. 8, no. 12, pp. 1610–1621, 2009.

[16] M. Erol, L. F. M. Vieira, and M. Gerla, "Localization with DiveNRise (DNR) beacons for underwater acoustic sensor networks," in *Proc. of ACM WUWNet*, 2007, pp. 97–100.

[17] M. Erol, L. F. M. Vieira, and M. Gerla, "AUV-aided localization for underwater sensor networks," in *Proc. of Wireless Algorithms, Systems and Applications*, 2007, pp. 44–54.

[18] M. Waldmeyer, H.-P. Tan, and W. K. G. Seah, "Multi-stage AUV-aided localization for underwater wireless sensor networks," in *Proc. of Adv. Information Net. and Applications*, 2011, pp. 908–913.

[19] T. Ojha and S. Misra, "HASL: High-speed AUV-based silent localization for underwater sensor networks," in *Proc. of QShine*. Greater Noida, India: Springer LNICST 115, 2013, pp. 128–140.

[20] T. Ojha and S. Misra, "MobiL: A 3-dimensional localization scheme for mobile underwater sensor networks," in *Proc. of National Conf. on Comm.*, New Delhi, India, 2013, pp. 1–5.

[21] W. Cheng, A. Y. Teymorian, L. Ma, X. Cheng, X. Lu, and Z. Lu, "Underwater localization in sparse 3D acoustic sensor networks," in *Proc. of IEEE INFOCOM*, 2008, pp. 236–240.

[22] H. D. Sherali, A. L. Soyster, and F. H. Murphy, "Stackelberg-Nash-Cournot Equilibria: Characterizations and computations," *Operations Research*, vol. 31, no. 2, pp. 253–276, 1983.

[23] W. Cheng, A. Thaeler, X. Cheng, F. Liu, X. Lu, and Z. Lu, "Time-synchronization free localization in large scale underwater acoustic sensor networks," in *Proc. of ICDCS Workshop*, 2009, pp. 80–87.

[24] N. Li and J. C. Hou, "Localized topology control algorithms for heterogeneous wireless networks," *IEEE/ACM Trans. on Networking*, vol. 13, no. 6, pp. 1313–1324, 2005.

[25] X. Chu and H. Sethu, "Cooperative topology control with adaptation for improved lifetime in wireless ad hoc networks," in *Proc. of IEEE INFOCOM*, Orlando, FL, USA, 2012, pp. 262–270.

[26] H. Sethu and T. Gerety, "A new distributed topology control algorithm for wireless environments with non-uniform path loss and multipath propagation," *Ad Hoc Networks*, vol. 8, no. 3, pp. 280–294, 2010.

[27] H. Ren and M.-H. Meng, "Game-theoretic modeling of joint topology control and power scheduling for wireless heterogeneous sensor networks," *IEEE/ACM Trans. on Automation Science and Engineering*, vol. 6, no. 4, pp. 610–625, 2009.

[28] A. Manolakos, V. Karyotis, and S. Papavassiliou, "A cross-layer-based topology control framework for wireless multihop networks," *IEEE Trans. on Vehicular Technology*, vol. 61, no. 6, pp. 2858–2864, 2012.

[29] L. Liu, R. Wanga, and F. Xiao, "Topology control algorithm for underwater wireless sensor networks using gps-free mobile sensor nodes," *J. of Network and Computer Applications*, vol. 35, pp. 1953–1963, 2012.

[30] T. Ojha, M. Khatua, and S. Misra, "Tic-Tac-Toe-Arch: A self-organizing virtual architecture for underwater sensor networks," *IET Wireless Sensor Systems*, vol. 3, no. 4, pp. 307–316, 2013.

[31] L. Berkhovskikh and Y. Lysanov, *Fundamentals of Ocean Acoustics*. Germany: Springer, 1982.

[32] A. Caruso, F. Paparella, L. F. M. Vieira, M. Erol, and M. Gerla, "The meandering current mobility model and its impact on underwater mobile sensor networks," in *Proc. of IEEE INFOCOM*, 2008, pp. 771–779.

[33] A. Sanchez, S. Blanc, P. Yuste, and J. J. Serrano, "A low cost and high efficient acoustic modem for underwater sensor networks," in *Proc. of IEEE/MTS OCEANS*, June 2011, pp. 1–10.

Dr. Sudip Misra is an Associate Professor in the School of Information Technology at the Indian Institute of Technology Kharagpur. He received his Ph.D. degree in Computer Science from Carleton University, Ottawa, Canada. His research interest is broadly on wireless networks. He has won 8 research paper awards in different conferences. He was awarded the IEEE ComSoc Asia Pacific Outstanding Young Researcher Award at IEEE GLOBECOM 2012. He was also awarded the Canadian Governments NSERC Post Doctoral Fellowship and the Humboldt Research Fellowship in Germany.

Tamoghna Ojha is a PhD candidate at the School of Information Technology, Indian Institute of Technology Kharagpur, India. He is also the co-founder and Director of SkinCurate Research Private Limited. Previously, Mr. Ojha completed MS degree from the Indian Institute of Technology Kharagpur in 2014. His research interests include mobile computing, ad-hoc and sensor networks, smart grids. He was the winner of GE Edison Challenge 2013.

Ayan Mondal is presently pursuing his M.S. degree from the School of Information Technology, Indian Institute of Technology Kharagpur, India. His current research interests include algorithm design for smart grid and wireless sensor networks. He received his B.Tech degree in Electronics and Communication Engineering from West Bengal University of Technology, India in 2012. Mr. Mondal is a student member of IEEE and ACM.